Donor–Acceptor Polymers: A Conjugated Oligo(*p*-Phenylene Vinylene) Main Chain with Dangling Perylene Bisimides

Edda E. Neuteboom, Paul A. van Hal, and René A. J. Janssen*[a]

Abstract: Two new donor–acceptor copolymers that consist of an enantiomerically pure oligo(*p*-phenylene vinylene) main chain with dangling perylene bisimides have been synthesized by using a Suzuki cross-coupling polymerization. Absorption and circular dichroism spectroscopy revealed that the transition dipole moments of the donor in the main chain and the dangling acceptor moieties of the copolymers are coupled and in a helical orientation in solution, even at elevated temperatures. A strong fluorescence quenching of both chromophores indicates an efficient photoinduced charge transfer after photoexcitation of either donor or acceptor. The formation and recombination kinetics of the charge-separated state were investigated in detail with femtosecond and near-steady-state photoinduced absorption spectroscopy. The charge-separated state forms within 1 ps after excitation, and recombination occurs with a time constant of 45–60 ps, both in solution and in the solid state. These optical characteristics indicate a short distance and appreciable interaction between the electron-rich donor chain and the dangling electron-poor acceptor chromophores.

Keywords: donor–acceptor systems · electron transfer · photochemistry · polymers · time-resolved spectroscopy

Introduction

An increasing number of polymers is being reported that contain donor and acceptor moieties incorporated in the main chain, as endgroups, pendant groups, or as block copolymers.[1–7] These donor–acceptor polymers are designed to enable energy and electron transfer in the electronically excited state of the polymer, and thereby create novel optoelectronic properties for application in light-emitting diodes and photovoltaic cells.

Especially in solar cells, mesoscopic ordering of donor and acceptor moieties is crucial for the creation of a photoactive layer that is able to convert absorbed photons efficiently into electrons and holes as well as for the subsequent transportation of these charges to the electrodes. One attractive strategy is the preparation of "double-cable" polymers.[8] These polymers consist of a conjugated donor main chain (donor "cable") bearing a number of closely spaced acceptor moieties (acceptor "cable"). Double-cable polymers are designed to ensure an intimate contact between donor and acceptor segments by avoiding extensive clustering and large-scale phase separation of the donor and acceptor phases, which may occur when the two individual moieties are mixed. By virtue of the covalently linked structure, a bicontinuous network on a molecular scale is formed. In photovoltaic devices based on double-cable polymers, holes are expected to move away from the electron acceptors by intrachain and interchain migration, while the electrons can hop between the acceptor units. The majority of double cable polymers reported in the literature have fullerene C_{60} as the dangling acceptor unit. These materials have been synthesized by either electrochemical polymerization,[9–12] chemical polymerization,[13,14] or by grafting a functionalized conjugated polymer with fullerene C_{60} moieties.[10,15,16] In addition to fullerene-based double-cable polymers, polythiophenes with pendant tetracyanoanthraquinodimethane moieties have been reported.[17,18] Although some of these double-cable polymers were incorporated in working photovoltaic devices,[13,14] their photophysical properties have not been studied on short timescales. Hence, the detailed kinetics of charge separation and recombination in double-cable polymers is unknown.

Recently, there has been an increasing interest in the incorporation of perylene bisimides as energy- or electron-acceptors with conjugated oligomers or polymers.[1–5,19–25] We have reported on the properties of two alternating copolymers of oligo(*p*-phenylene vinylene) (OPV) and perylene bisimide that exhibit an efficient charge separation in solution and in the solid state.[26] The photophysical properties

[a] Dr. E. E. Neuteboom, Dr. P. A. van Hal, Prof. R. A. J. Janssen
Molecular Materials and Nanosystems
Eindhoven University of Technology
P.O. Box 513 5600 MB Eindhoven (The Netherlands)
Fax: (+31)40-2451036
E-mail: R.A.J.Janssen@tue.nl

 DOI: 10.1002/chem.200400097

in the solid state indicated that these polymers form stacks of alternating OPV and perylene bisimide units in the solid state as a result of favorable interactions of the electron-rich donor moieties with the electron-poor acceptor units, similar to the *Aeda*mers (*a*romatic *e*lectron *d*onor *a*cceptor-mers) pioneered by Lokey and Iverson.[27] Another attempt to mesoscopically organize OPV and perylene bisimide chromophores has been reported for a triad consisting of two tridodecyloxy-OPV units attached to a central perylene bisimide core that possesses a liquid-crystalline mesophase and, hence, provides a handle to achieve ordered morphologies upon annealing.[28] Indeed, charge recombination was reduced in more ordered phases as a consequence of improved charge transport. Changing the polymer architecture from a linear array of alternating donors and acceptors to a conjugated donor main chain with pendant acceptors, could induce differences in the photophysical properties. With this in mind, new polymers involving OPV and perylene bisimide were designed.

Herein we present the synthesis and photophysical properties of two new copolymers (**P1** and **P2**, Scheme 1) that consist of enantiomerically pure OPV donor segments in the main chain alternating with phenylenes carrying a pendant perylene bisimide acceptor. These polymers differ with respect to the substitution pattern of the phenylene ring connecting two OPV units. For **P1**, the OPV units are placed in the *para* positions with respect to each other, while in **P2** they are in a *meta* configuration.

Results and Discussion

Synthesis: To synthesize polymers **P1** and **P2**, two different perylene bisimide co-monomers were prepared that were subsequently allowed to react with an OPV monomer in a Suzuki polymerization.

The first step in the synthesis of the chiral perylene bisimide co-monomer for **P1** (Scheme 2) was the Williamson etherification of 2,5-dibromobenzene-1,4-diol (**1**)[29] with racemic 2-ethylhexyl bromide, yielding alcohol **2**. Subsequently, alcohol **2** was coupled under Mitsunobu conditions with enantiomerically pure *tert*-butyl ((*S*)-1-hydroxymethyl-3-methylbutyl)carbamate (**3**)[26] to the butoxycarbonyl (BOC)-protected diether **4**, which was deprotected with trifluoroacetic acid (TFA) and $NaHCO_3$ to afford the free amine **5**. *N*,*N*′-Bis(1-ethylpropyl)perylene-3,4:9,10-tertacarboxylic-bisimide (**6**)[30] was partially hydrolyzed with potassium hydroxide in *tert*-butyl alcohol to the anhydride imide **7**.[31,32] The final reaction of amine **5** with monoanhydride **7** resulted in perylene bisimide **8**, which was obtained as a mixture of two diastereomers.

The perylene bisimide co-monomer for **P2** (Scheme 3) was synthesized starting with a Mitsunobu reaction of 2,4-dibromophenol (**9**) with alcohol **3** that lead to the formation of ether **10**. After deprotection of **10** with TFA and $NaHCO_3$, amine **11** was treated with the anhydride **7** to afford the perylene bisimide **12**. Monomer **13**, which is used as a reference compound for monomer **12**, was obtained by a Williamson etherification of phenol **9** with racemic 2-ethylhexyl bromide.

In all polymerization reactions, bisboralane (*E*,*E*)-1,4-bis{4-{4,4,5,5-tetramethyl[1,3,2]dioxaborolan-2-yl-}-2,5-bis[(*S*)-2-methylbutoxy]styryl}-2,5-bis[(*S*)-2-methylbutoxy]-benzene (**14**)[26] was allowed to react with the chosen dibromoaryl co-monomer in a palladium-catalyzed Suzuki reaction (Scheme 4). Reaction of co-monomer **14** with perylene bisimide co-monomers **8** and **12** resulted in the formation of perylene bisimide-substituted polymers **P1** and **P2**, respectively. Likewise, polymerization of **14** with 1,4-dibromo-2,5-di(2-ethylhexyloxy)benzene (**15**)[33,34] and **13** provided the corresponding reference polymers **RP1** and **RP2** that have the same main chains as **P1** and **P2**; however, they lack the dangling perylene bisimide chromophores. The polymers were characterized by ^1H and ^{13}C NMR spectroscopy, and size-exclusion chromatography (SEC). The molecular weights and polydispersities (PDI), determined by SEC in chloroform versus polystyrene standards, are $M_n = 8.2\,kg\,mol^{-1}$ for **P1** and $M_n = 8.0\,kg\,mol^{-1}$ for **P2** and a

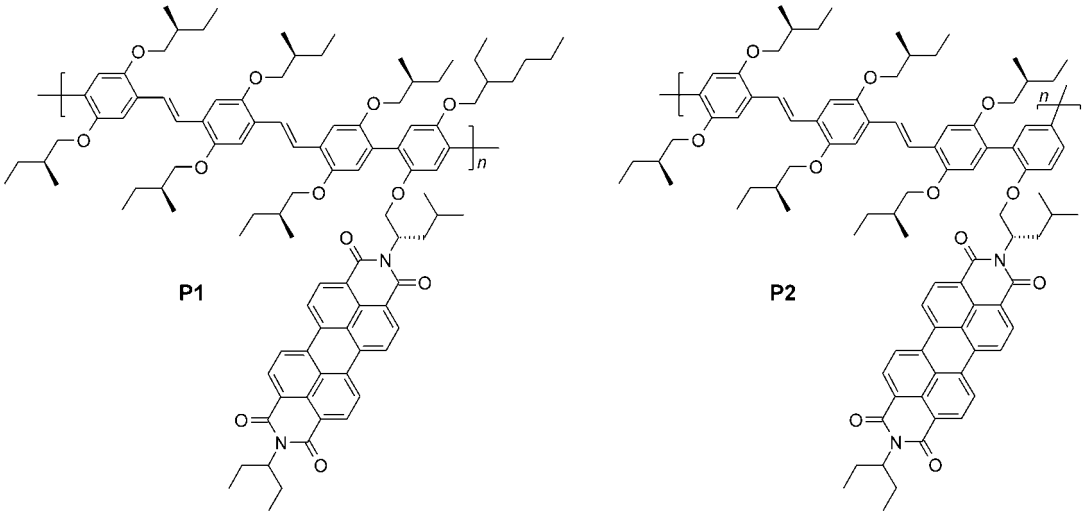

Scheme 1. Structures of donor–acceptor copolymers **P1** and **P2**.

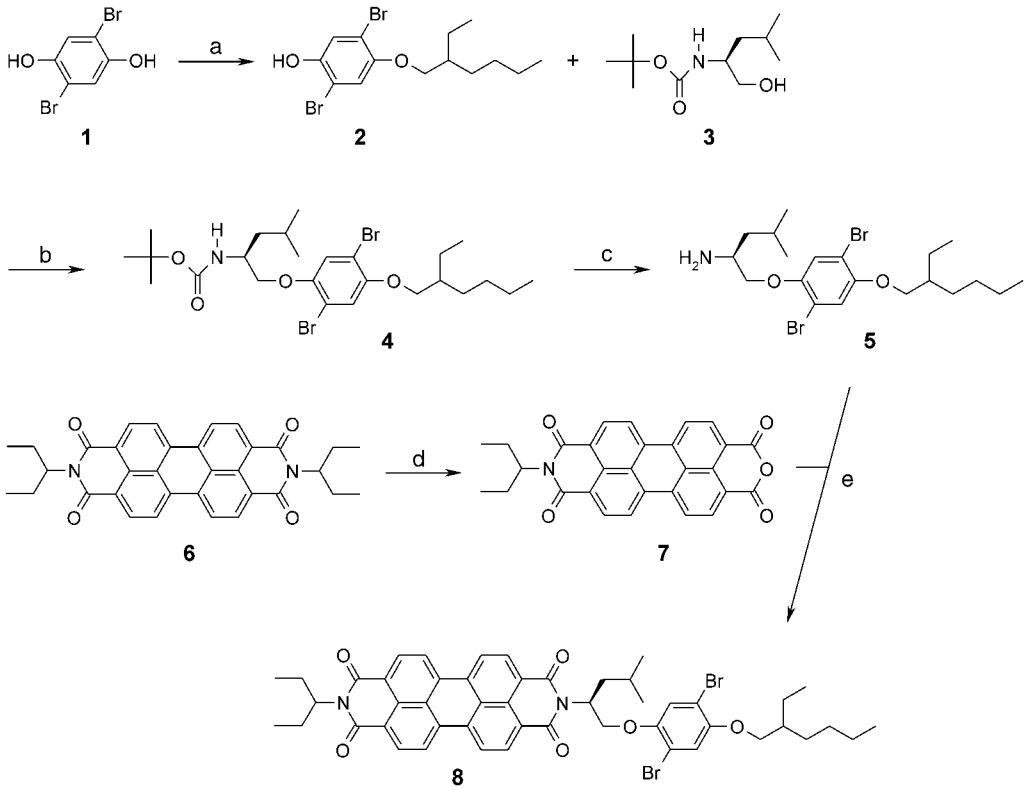

Scheme 2. Synthesis of the perylene bisimide monomer **8**: a) K_2CO_3, 2-ethylhexyl bromide, ethanol, reflux, 28%; b) PPh_3, DEAD, toluene, 36%; c) i) TFA, CH_2Cl_2; ii) $NaHCO_3$, 91%; d) KOH, *t*BuOH, 20%; e) DMF, 155°C, 39%.

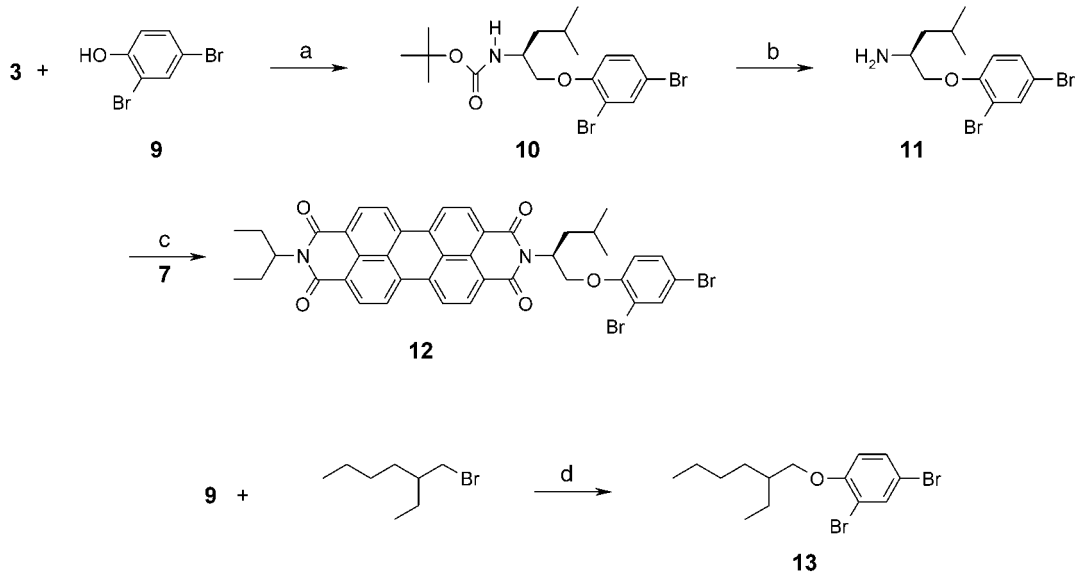

Scheme 3. Synthesis of the perylene bisimide monomer **12** and the reference monomer **13**: a) PPh_3, DEAD, toluene, 28%; b) i) TFA, CH_2Cl_2; ii) $NaHCO_3$, 83%; c) DMF, 160°C, 69%. d) K_2CO_3, ethanol, reflux, 24%.

PDI of 3.3 and 2.8, respectively. Hence these polymers have a rather low degree of polymerization (n = 5–6 units). The reference polymers have higher molecular weights of M_n = 24.6 kg mol^{-1} (**RP1**, PDI = 4.5, n = 22) and M_n = 13.8 kg mol^{-1} (**RP2**, PDI = 3.5, n = 14), with a correspondingly higher degree of polymerization. The reason for the difference with respect to M_n of the donor–acceptor polymers and the reference polymers is not known; however, the solubility of the polymers might play a role because the products precipitate in the reaction mixture. The integrals of the ^{1}H NMR spectra show that the perylene bisimide monomers (or their respective reference monomers) and the OPV monomer are incorporated in an equimolar fashion in all four polymers.

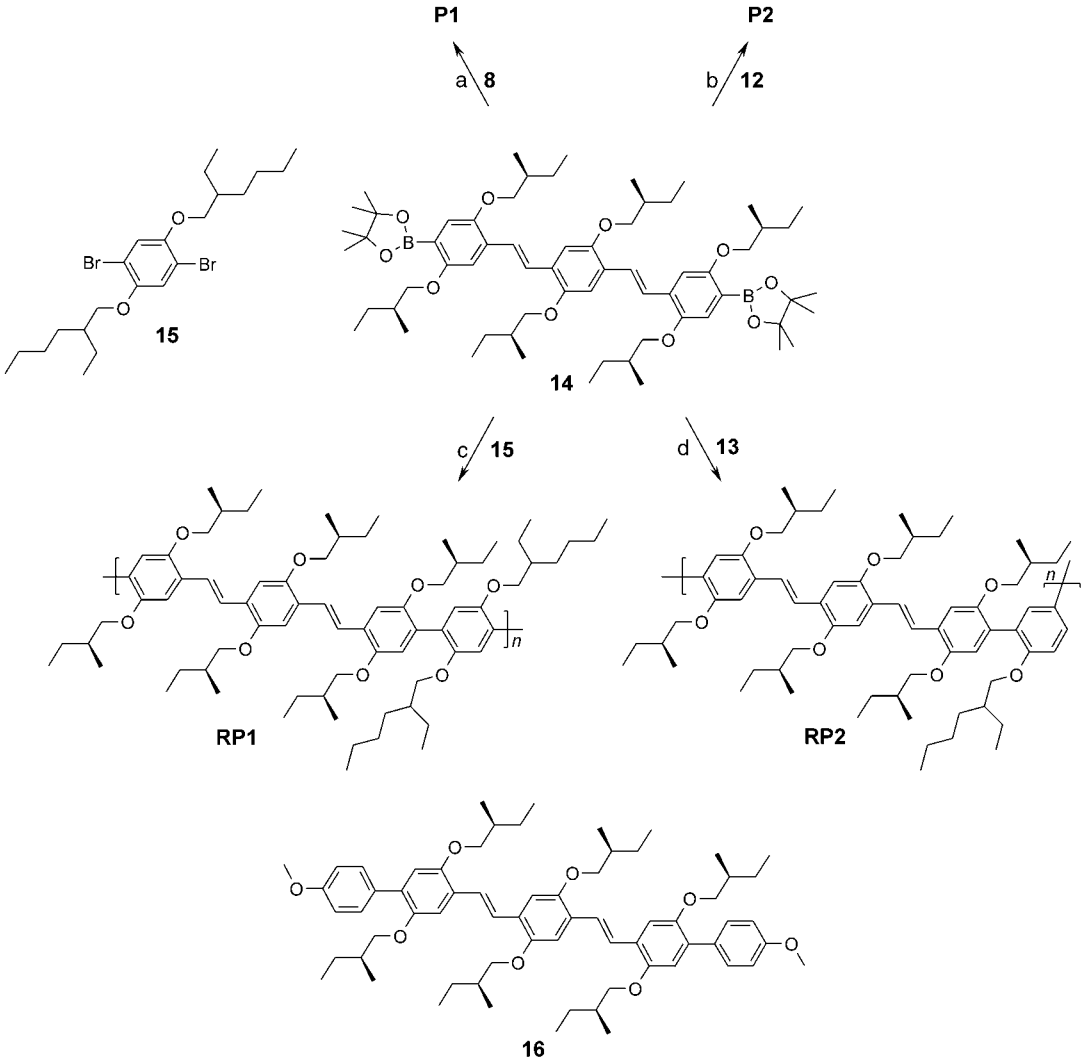

Scheme 4. Overview of the synthesis of the perylene bisimide-substituted polymers **P1** and **P2**, their reference polymers **RP1** and **RP2**, and the structure of model compound **16**. a) $[Pd(PPh_3)_4]$, K_2CO_3, water, THF, 90 °C, 72 %; b) $[Pd(PPh_3)_4]$, K_2CO_3, water, THF, 90 °C, 75 %; c) $[Pd(PPh_3)_4]$, K_2CO_3, water, THF, 90 °C, 51 %; d) $[Pd(PPh_3)_4]$, K_2CO_3, water, THF, 90 °C, 55 %.

Absorption spectra in solution: The polymers and model compound **6** were also characterized with UV/Visible absorption spectroscopy in toluene solution (Figure 1). The perylene bisimide segment (PERY) absorbs at $\lambda = 458$ nm, 489 nm and 526 nm, as demonstrated by **6**. The maximum of the absorption of **RP1** at $\lambda = 431$ nm is slightly red-shifted compared to that of **RP2** at 426 nm, as a result of the different topology at the phenylene rings connecting the OPV segments. In **RP1**, the *para*-phenylene ring causes a slightly more effective conjugation of the adjacent OPV segments than in **RP2**, in which the OPV segments are linked by *meta*-phenylene. The absorption spectra of **P1** and **P2** clearly show that both the OPV backbone and the perylene bisimide are incorporated. It seems, however, that in both cases the absorption intensity in the 400–470 nm region is too high compared to the perylene absorption at 528 nm. It is unlikely that this is caused by to a significant deviation from the equimolar incorporation of the OPV and perylene bisimide monomers in the polymer chain because ^{1}H NMR spectroscopy confirmed that their ratio is 1:1 in **P1** and **P2**. A possible explanation is an electronic interaction between the two chromophores, which was also observed for a macrocycle containing exactly one OPV and one perylene bisimide that shows the same deviation.[26] When the two chromophores are in close proximity and the angle between their transition dipole moments is less than the magic angle of 54.7°, exciton coupling will increase the probability of the high-energy transition of the OPV segments compared to that of the low-energy transition of the perylene bisimide, resulting in increased absorption at lower wavelengths. Because of the flexible linker between the backbone and the perylene bisimides, such electronic coupling is also possible in polymers **P1** and **P2**. Absorption spectra in toluene were recorded as a function of the temperature in the range from 20 to 90 °C, with heating steps of 10 °C (Figure 2a,c). The UV/Vis spectra show a small blue shift with increasing temperature, which is commonly observed for dialkoxy-substituted PPVs.[35] In addition, the intensity of the band at $\lambda \approx$ 430 nm decreases slightly relative to the band at $\approx$530 nm. This might indicate a decreasing electronic interaction. The

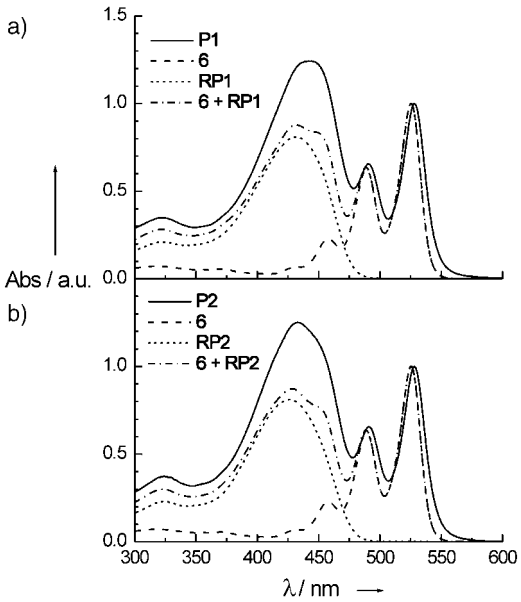

Figure 1. Absorption spectra in toluene of a) **P1**, **6**, **RP1**, and b) **P2**, **6**, **RP2** together with the 1:1 summation of the spectra of the reference polymers and **6**. The spectra are normalized at ~527 nm. The spectra of **RP1** and **RP2** are normalized with respect to the normalized spectra of the summation spectra.

spectral changes observed on changing the temperature are fully reversible because the original spectra at 20 °C were recovered after cooling the sample from 90 °C.

Circular dichroism spectra in solution: The stereochemistry of **P1** and **P2** can be used to address the electronic interaction between the perylene bisimide and the enantiomerically pure OPV segments by circular dichroism (CD) spectroscopy in more detail. In these polymers, an exciton coupling between main-chain OPV segments and the pendant chromophores will result in a CD signal when the transition dipole moments are in a preferential helical orientation with respect to each other. In this case, the preferential helicity can originate from the interaction between the perylene bisimide, having an enantiomerically pure (*S*)-leucinoxy linker to the backbone, and the OPV with its enantiomerically pure (*S*)-2-methylbutoxy sidechains. The CD spectra of the polymers **P1** and **P2** were recorded in toluene as a function of the temperature in heating steps of 10 °C, starting at 20 °C and ending at 90 °C (Figure 2b,d). Both polymers exhibit a negative CD signal at the absorption of the OPV segments and a positive CD signal at the perylene bisimide absorption. This indicates exciton coupling between the donor and the acceptor chromophores with a positive helicity, namely, a right-handed rotation will superimpose the two transition dipole moments (which are essentially parallel to the long axis in both chromophores). This effect has also been observed for an OPV-perylene bisimide macrocycle, which exhibited a similar spectrum.[26] As the temperature increases, the CD spectra maintain their shape but become gradually less intense. As in the absorption experiments, the temperature-dependent CD measurements were also reversible. The combined data from the UV/Vis and CD spectra indicate

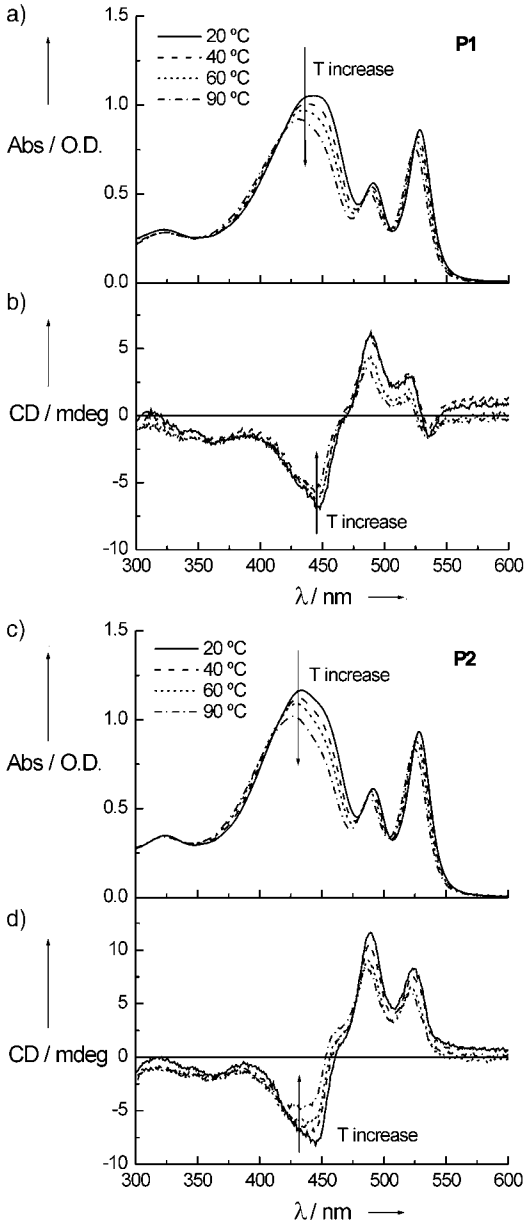

Figure 2. Temperature dependence of the UV/Vis absorption (a and c) and circular dichroism spectra (b and d) of solutions of **P1** (a,b) and **P2** (c,d) in toluene, recorded upon heating from 20 °C to 90 °C in steps of 10 °C.

that the two chromophores are in relatively close proximity, probably as a consequence of the stacking propensity of the donor chain and the dangling acceptors, with their transition dipole moments in a right-handed helical orientation with an angle of less than 54.7°.

In fact, polymers **P1** and **P2** exhibit somewhat different CD effects for the perylene bisimide manifold. **P1** shows a small bisignated signal at $\lambda \approx 530$ nm that points to an additional perylene–perylene coupling. A different interaction between the chromophores in the *meta*- versus *para*-connected systems may be considered as a tentative explanation for this difference. A more detailed understanding can probably be obtained by investigating the diastereomers of **P1**

and **P2**. In this respect, it is important to mention that although **P1** and **P2** contain enantiomerically pure (*S*)-2-methylbutoxy side chains on the OPV unit and a (*S*)-leucinol linker at the perylene bisimide, there are some subtle stereochemical differences. **P1** was synthesized from co-monomers **12** and **14** that resulted in a stereochemical irregularity along the polymer chain because racemic 2-ethylhexyl side chains are used in **14**. This stereochemical aspect does not apply to the polymer **P2** because its co-monomer **12** contains only one stereocenter.

Energetics of charge separation: Before addressing the photoinduced charge separation in polymers **P1** and **P2** experimentally, it is instructive to consider the thermodynamics of such a process. In general, the Gibbs free energy of an intramolecular charge-separated state (G_{CS}) in a covalently bonded donor–acceptor system can be estimated from the Weller equation.[36]

$$G_{CS} = e[E_{ox}(D)-E_{red}(A)] - \frac{e^2}{4\pi\varepsilon_0\varepsilon_s R_{cc}} - \frac{e^2}{8\pi\varepsilon_0}\left(\frac{1}{r^+}+\frac{1}{r^-}\right)\left(\frac{1}{\varepsilon_{ref}}+\frac{1}{\varepsilon_s}\right) \quad (1)$$

To obtain G_{CS}, the first reduction potential $E_{red}(A)$ of compound **6** (−0.65 V versus SCE) in dichloromethane (ε_{ref} = 8.93) and the first oxidation potential $E_{ox}(D)$ of OPV model compound **16** (+0.80 V versus SCE) were used.[26] Although the backbones of **P1** and **P2** are more extended, a comparison with **16** is justified because the absorption spectra are very similar (λ_{max} = 425 nm for **16**), which indicates that the conjugation length in the polymers **P1** and **P2** is comparable to that of **16**. The radius of the PERY anion (r^- = 4.7 Å) was estimated from the density (ρ = 1.59 g cm^{-3}) of *N*,*N*′-dimethylperylene-3,4:9,10-tetracarboxylic-bisimide and from the X-ray crystallographic data with $r^- = [3M/(4\pi\rho N_A)]^{1/3}$.[37] The radius of the positive ion of the OPV segment was estimated in a similar way to be r^+ = 5.1 Å.[38] The distance between the centers of the donor and acceptor segments R_{cc} was estimated by means of molecular modeling to be within the range of 4 to 16 Å for both **P1** and **P2**. This wide range of distances is a consequence of the flexible spacer connecting the phenylene ring of the backbone and the perylene bisimide. Substitution of these parameters in Equation (1) shows that the intramolecular charge-separated state in the polymers in toluene (ε_s = 2.38) is lower than the energy of the OPV and PERY singlet excited states determined from the 0–0 transition of the fluorescence (S_1 OPV = 2.56 eV, S_1 PERY = 2.32 eV, Table 1). In fact, ΔG_{CS} would still be negative up to a donor–acceptor distance of 150 Å, which is much larger than the actual distance that can occur in these two polymers. The estimates show that electron transfer in **P1** and **P2** is an exergonic reaction, irrespective of whether it originates from the OPV or perylene bisimide S_1 states.

Fluorescence spectra and fluorescence quenching in solution: The occurrence of an intramolecular photoinduced electron transfer in **P1** and **P2** was studied experimentally by fluorescence spectroscopy in toluene (Figure 3) and

Table 1. Free energy of intramolecular and intermolecular charge-separated states calculated from Equation (1) (see text for parameters used) in toluene relative to the ground state and the singlet-excited state of OPV and PERY.

		$\Delta G_{CS} = G_{CS} - E_{00}$	
R_{cc} [Å]	G_{CS} [eV]	S_1 OPV [eV]	S_1 PERY [eV]
4	0.85	−1.71	−1.47
16	1.98	−0.57	−0.34
150	2.32	−0.24	0
∞	2.36	−0.20	0.04

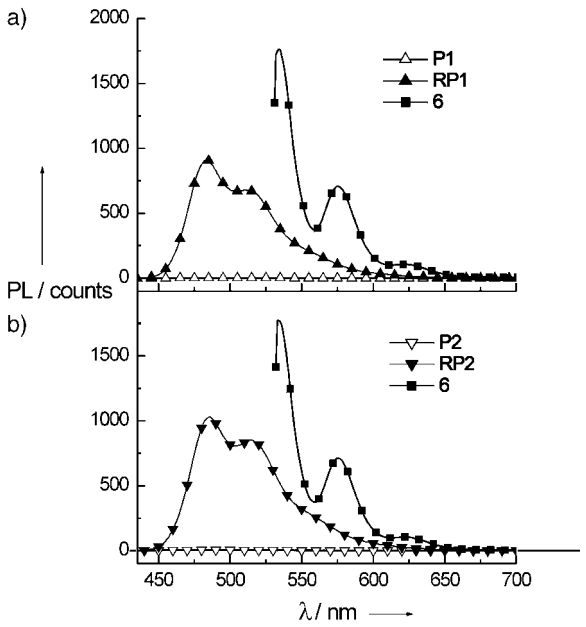

Figure 3. Fluorescence emission spectra in toluene of a) polymers **P1** and **RP1** upon excitation at λ = 433 nm and compound **6** upon excitation at λ = 529 nm, and of b) polymers **P2** and **RP2** upon excitation at λ = 427 nm and **6** upon excitation at λ = 529 nm. The spectra are corrected for the optical density at the excitation wavelength.

ortho-dichlorobenzene (ODCB). In these experiments, **P1** and **P2** were excited at either λ = 433 nm or 427 nm, and at 529 nm, to ensure (almost) selective excitation of the OPV segments and the perylene bisimide chromophores, respectively. The fluorescence intensity was compared to the fluorescence of the reference compounds **RP1**, **RP2**, and **6** (λ_{max} = 482–485 nm, 485–486 nm, and 534 nm respectively), which were excited at the same wavelengths as **P1** and **P2**. The quenching factors *Q* were determined by comparing the fluorescence intensities of the OPV and perylene bisimide chromophores of **P1** and **P2** with those of **RP1**, **RP2**, and **6** at the wavelengths of maximum emission. In toluene, the fluorescence quenching factors for **P1** are Q_{OPV} = 390 (compared to **RP1**) and Q_{PERY} = 540 (compared to **6**), while **P2** exhibited quenching factors of Q_{OPV} = 200 (compared to **RP2**) and Q_{PERY} = 440 (compared to **6**). In ODCB, the quenching is similar with Q_{OPV} = 280 and Q_{PERY} = 600 for **P1**, and Q_{OPV} = 200 and Q_{PERY} = 400 for **P2**.

The almost complete quenching of the fluorescence of both chromophores demonstrates that an efficient charge

separation takes place in **P1** and **P2** after excitation of the OPV segments in the backbone or the pendant perylene bisimides. It is important to note that the small residual fluorescence of **P1** and **P2** may originate from minute amounts (<0.5%) of highly fluorescent impurities, such as monomers, and therefore the quenching factors for **P1** and **P2** should not be taken as absolute values, but should be considered to be a lower limit of the actual numbers.

As shown in Figure 4, excitation of the OPV segment to its S_1 state may result in the direct formation (k_{CS}^d) of a charge-separated state (CSS) or in an indirect formation of

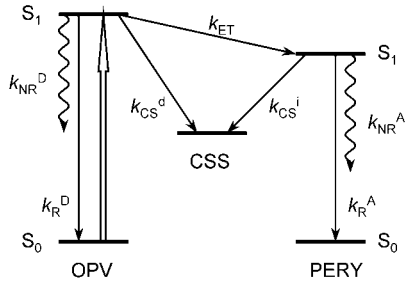

Figure 4. Jablonski diagram representing the different photophysical events that can take place in the donor–acceptor (D–A) polymers **P1** and **P2** upon excitation of the OPV backbone (open arrow). The singlet energy transfer (k_{ET}), the direct (k_{CS}^d) and indirect (k_{CS}^i) electron transfer, the radiative emission (k_R) and non-radiative emission (k_{NR}) are indicated.

CSS via singlet-energy transfer (k_{ET}) to an intermediate perylene bisimide S_1 state, followed by charge transfer (k_{CS}^i). Of course, direct excitation of perylene bisimide also gives CSS, with a rate constant k_{CS}^i. It is possible to estimate the rate constants for charge separation by the direct and indirect pathways (k_{CS}^d and k_{CS}^i) and the rate of energy transfer (k_{ET}) from fluorescence quenching Q (Table 2). The sum of k_{ET} and k_{CS}^d can be estimated with Equation (2) from the OPV fluorescence quenching (Q_{OPV}) and the fluorescence lifetime of the OPV segments τ_{OPV} ($= (k_R^D + k_{NR}^D)^{-1}$) (Figure 4), which equals 0.9 ns for **RP1** and 1.1 ns for **RP2** in toluene (determined by time-correlated single-photon counting).

$$k_{ET} + k_{CS}^d = \frac{Q_{OPV}-1}{\tau_{OPV}} \quad (2)$$

Thus $k_{ET} + k_{CS}^d = 4.3\times10^{11}\,s^{-1}$ for **P1** and $k_{ET} + k_{CS}^d = 1.8\times10^{11}\,s^{-1}$ for **P2**. Similarly, k_{CS}^i can be estimated from the fluorescence quenching after selective excitation of the perylene bisimide (Q_{PERY}) and the fluorescence lifetime τ_{PERY} = 4 ns of compound **6**[26] by means of Equation (3). This gives $k_{CS}^i = 1.3\times10^{11}\,s^{-1}$ for **P1** and $k_{CS}^i = 1.1\times10^{11}\,s^{-1}$ for **P2**, both in toluene.

$$k_{CS}^i = \frac{Q_{PERY}-1}{\tau_{PERY}} \quad (3)$$

Because the quenching factors are lower limits, these rates must also be considered as lower estimates.

Photoinduced absorption in solution: The charge-separated state can also be monitored by transient photoinduced absorption (PIA) spectroscopy. In order to investigate the charge separation and recombination processes, toluene solutions of **P1** and **P2** were studied by time-resolved femtosecond pump-probe spectroscopy. The polymers were excited with a ~150 fs pulse at 450 nm or 525 nm to distinguish between processes occurring from either donor or acceptor excitation.

Figure 5 shows the normalized transient change in transmission $\Delta T/T$ at 1450 nm (0.86 eV) as a function of the time delay between the pump and probe pulses arriving at the

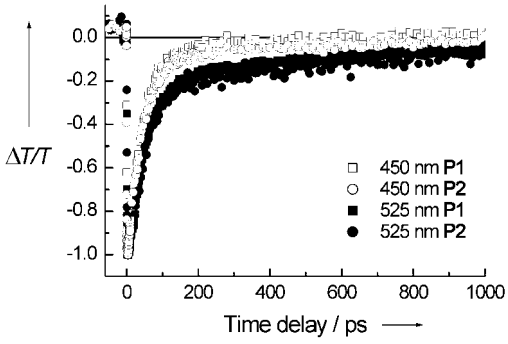

Figure 5. Normalized differential transmission dynamics of toluene solutions of **P1** and **P2** at room temperature, recorded at λ = 1450 nm (low-energy absorption of OPV radical cations) after excitation at λ = 450 nm and 525 nm.

sample. The probe wavelength of 1450 nm corresponds to the $D_0 \rightarrow D_1$ absorption of the doublet state $OPV^{+\cdot}$ radical cation and, hence, monitors the formation and decay of the charge-separated state. The negative value of $\Delta T/T$ is consistent with an absorption attributed to $OPV^{+\cdot}$ radical cations, which are formed within 0.5 ps ($k_{CS} \geq 2\times10^{12}\,s^{-1}$) after arrival of the pump pulse. For both polymers, the recombination time constant is ~45 ps for time delays of 0–250 ps after excitation at 450 nm. When the perylene bisimide chromophores of **P1** and **P2** are selectively excited at 525 nm, charge separation is equally fast, whereas recombination appears to be slightly slower, resulting in a lifetime of ~60 ps.

Table 2. Rate constants for energy transfer, direct and indirect charge separation, and charge recombination as obtained from photoluminescence quenching and pump-probe PIA spectroscopy for **P1** and **P2** in toluene solutions and the solid state.

		PL quenching[a]				PIA OPV		PIA PERY	
		Q_{OPV}	Q_{PERY}	$k_{ET}+k_{CS}^d$ [ns^{-1}]	k_{CS}^i [ns^{-1}]	k_{CS}^i or $k_{ET}+k_{CS}^d$ [ns^{-1}]	k_{CR} [ns^{-1}]	k_{CS}^i [ns^{-1}]	k_{CR} [ns^{-1}]
P1	toluene	390	540	430	130	≥2000	22	≥2000	18
	film					≥2000	18	≥2000	16
P2	toluene	200	440	180	110	≥2000	22	≥2000	16
	film					≥2000	16	≥2000	18

[a] Rate constants determined from PL quenching are lower limits to the actual values as explained in the text.

In a control experiment, pump-probe spectroscopy was performed on **RP1**, **RP2**, and compound **6** in toluene. Again, the solutions were excited at 450 nm (**RP1** and **RP2**) and 525 nm (**6**), and probed at 1450 nm. The intensities obtained for all three solutions are lower by a factor of 5–10 compared to those of **P1** and **P2**, and the signals have much longer decay constants. Therefore, the transient signals of **RP1**, **RP2**, and **6** probably correspond to an excited-state $S_1 \rightarrow S_n$ absorption, whose lifetime corresponds to either τ_{OPV} or τ_{PERY}. The very different intensities and lifetimes of the photoinduced absorptions at 1450 nm of **P1** and **P2**, compared to the control experiments, support our assignment that they originate from an intramolecular charge-separated state.

Pump-probe measurements can give reliable rate constants for charge separation and recombination, although they are limited by the width of the excitation pulse. A comparison of the rates of charge separation measured by pump-probe spectroscopy $k_{CS} \geq 2 \times 10^{12}\ s^{-1}$ with the values of $k_{ET} + k_{CS}^{d}$ and k_{CS}^{i} ($1–4 \times 10^{11}\ s^{-1}$), obtained from fluorescence quenching, reveals that they are in satisfactory agreement, particularly if account is taken of the fact that the fluorescence quenching experiments are sensitive to impurities and therefore provide lower estimates.

The rate constants for charge separation were independent of the excitation wavelength (450 or 525 nm). This suggests that an ultrafast singlet energy transfer from the singlet excited state of OPV to the perylene bisimide moiety precedes the electron transfer, which originates from perylene bisimide singlet excited state S_1. However, it is not possible to make an unambiguous conclusion on the prevailing mechanism because the measured rates for charge separation are limited by the resolution of the pump-probe set-up.

Photoinduced absorption in the solid state: In the solid state it was possible to study the process of photoinduced charge transfer on long (microsecond to millisecond) and short (sub-picosecond to nanosecond) timescales by the use of different PIA set-ups. Near-steady-state PIA spectra of thin films of **P1** and **P2** on quartz were recorded at 80 K with excitation at 458 nm (Figure 6). The distinct absorptions of the $PERY^{-\bullet}$ radical anions at 1.28, 1.54, and 1.72 eV are clearly visible in the spectra.[39] The absorptions at 0.70 eV and in the region of 1.5–2.1 eV are attributed to $OPV^{+\bullet}$ radical cations, based on previous results for $OPV3^{+\bullet}$ and $OPV4^{+\bullet}$.[40] The 1.5–2.1 eV absorption of $OPV^{+\bullet}$ overlaps with the absorptions of the $PERY^{-\bullet}$ radical anions.

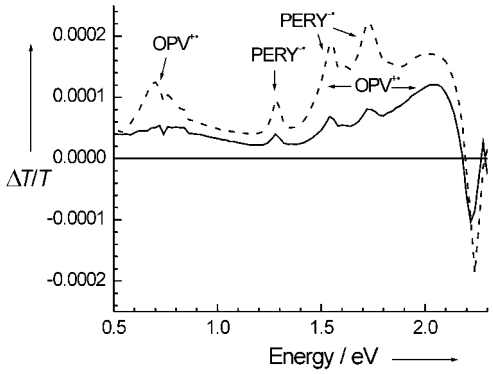

Figure 6. Near-steady-state photoinduced absorption spectra of **P1** (——) and **P2** (– – –) as thin films on quartz recorded at 80 K. The excitation wavelength is 458 nm, modulation frequency 275 Hz.

The PIA signals at 0.70 and 1.54 eV of both **P1** and **P2** in Figure 6 show a sublinear dependence with increasing intensity of the excitation. When the data are fitted to a power-law expression for ΔT as function of the pump intensity, exponents between 0.38 and 0.47 are obtained. This indicates that the charged species associated with these signals probably decay via a bimolecular recombination mechanism, for which an exponent of 0.5 would be expected. Exponents of less than 0.5 can be explained when the steady-state concentration of charges is trap-limited.[41] The signal intensities at 0.70 eV and 1.54 eV for **P1** and **P2** were found to decrease with increasing modulation frequency in an identical fashion, closely following a power-law decay with the modulation frequency. This indicates that the signals in the spectrum have the same origin and that a distribution of lifetimes exists in the solid state, extending into the millisecond time domain. The distribution of lifetimes is consistent with a trap-filling model for the long-lived charges observed in this experiment.

The actual charge formation and recombination processes in films of **P1** and **P2** were studied with respect to time at room temperature by femtosecond pump-probe spectroscopy (Figure 7). The pump wavelengths were 450 or 525 nm

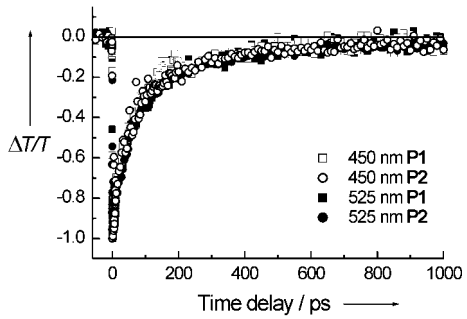

Figure 7. Normalized differential transmission dynamics of films of **P1** and **P2** at room temperature, recorded at $\lambda = 1450$ nm (low-energy absorption of OPV radical cations) after excitation at $\lambda = 450$ nm and 525 nm.

and the signals were probed at 1450 nm (0.86 eV). The charge formation and recombination kinetics of **P1** and **P2** are similar and independent of the excitation wavelengths. As in solution (Figure 5), the grow-in of the photoinduced absorption signals occurs extremely fast and is complete within 1 ps. The recombination of the positive and negative charges between 0 and 250 ps after charge formation occurs with a time constant of ≈ 60 ps. This lifetime corresponds to the value obtained for the solutions excited at 525 nm. The much longer lifetimes observed in the near-steady-state experiments are attributed to charges that escape from this fast geminate recombination by diffusion to different sites

on the same polymer chain or different chains, and stabilization owing to the low temperature (80 K).

Conclusion

Two new copolymers consisting of a main chain of enantiomerically pure OPV segments alternating with phenylenes with pendant perylene bisimides have been synthesized and studied. Photoluminescence quenching shows that an efficient photoinduced charge transfer takes place between the donor backbone and its pendant acceptors in toluene and ODCB solutions. In accordance with estimated values for the Gibbs free energy or charge separation, charge separation occurs irrespective of which of the two chromophores is initially excited. Femtosecond pump-probe spectroscopy on these polymer solutions allowed the rate of formation of the $OPV^{+\cdot}$ radical cations to be monitored. Charge separation occurs within 1 ps and the charge-separated state decays with a time constant of 45–60 ps. The time constants for charge separation and recombination in the solid state are similar to those in solution. This suggests that the relative orientation of the OPV and perylene bisimide chromophores in solution is similar to that in the solid state. UV/Vis and CD spectra reveal that the transition dipole moments of the OPV and perylene bisimide are coupled. This implies that these chromophores are in close proximity and have a preferential helical orientation. The combination of these results suggests that, both in solution and in films, the OPV and perylene bisimide are in close proximity owing to stacking of the electron-rich and electron-poor segments. This configuration enables fast and efficient charge separation, and eventually fast charge recombination. Such a fast recombination is probably not advantageous for the preparation of photovoltaic cells, where long lifetimes enhance the chances for charge collection. On the other hand, the rapid response and relaxation may open possibilities for the materials to be used in optical data processing.

Experimental Section

General methods: THF was freshly distilled over potassium/sodium. ^{1}H NMR and ^{13}C NMR spectra were recorded at room temperature on a Varian Gemini 300 or a Varian Mercury 400 MHz spectrometer. Chemical shifts are given relative to tetramethylsilane. Matrix-assisted laser desorption ionization time-of-flight (MALDI-TOF) mass spectrometry was conducted on a Perseptive Biosystems Voyager DE-Pro MALDI-TOF mass spectrometer. A Shimadzu LC-Chemstation 3D (HP 1100 Series) with a Polymer Laboratories MIXED-D column (particle size 5 μm; length/i.d. (mm): 300 × 7.5) and UV detection was employed for size-exclusion chromatography (SEC), with $CHCl_3$ as the eluent (1 mL min^{-1}). Elemental analyses were carried out on a Perkin-Elmer 2400 series II CHN analyzer.

UV/Vis absorption spectra were recorded on a Perkin Elmer Lambda 900 and a Lambda 40 spectrophotometer. Fluorescence spectra were recorded on an Edinburgh Instruments FS920 double-monochromator spectrometer and a Peltier-cooled red-sensitive photomultiplier. Circular dichroism spectra were recorded on a Jasco J-600 spectropolarimeter.

Fluorescence lifetimes: Time-correlated single-photon counting fluorescence studies were performed with an Edinburgh Instruments LifeSpec-PS spectrometer, consisting of a 400 nm picosecond laser (PicoQuant PDL 800B), operated at 2.5 MHz, and a Peltier-cooled Hamamatsu microchannel plate photomultiplier (R3809U-50). The Edinburgh Instruments software package was used to determine the lifetimes from the data.

Photoinduced absorption spectroscopy: Near-steady-state photoinduced absorption (PIA) spectra were recorded between 0.25 and 3 eV by excitation of a thin drop-cast film on quartz in an Oxford Optistat continuous flow cryostat with a mechanically modulated (typically 275 Hz) cw Ar-ion laser (Spectra Physics 2025) pump beam tuned to 458 nm (25 mW, beam diameter of 2 mm) and monitoring the resulting change in transmission (ΔT) of a tungsten-halogen white-light probe beam after dispersion by a triple grating monochromator, with Si, InGaAs, and (cooled) InSb detectors.

The femtosecond laser system used for pump-probe experiments consists of an amplified Ti-sapphire laser (Spectra Physics Hurricane) that provides 150 fs pulses at 800 nm with an energy of 750 μJ at 1 kHz. Pump (450 nm or 525 nm, fluence 0.5 μJ mm^{-2}) and probe (1450 nm) pulses were created by optical parametric amplification and twofold frequency doubling with two OPAs (Spectra Physics OPA-C). The pump beam was linearly polarized at the magic angle (54.7°) with respect to the probe beam. The temporal evolution was recorded with an InGaAs detector and standard lock-in detection at 500 Hz.

2,5-Dibromo-4-(2-ethylhexyloxy)phenol (2): 2,5-Dibromo-benzene-1,4-diol (**1**, 1.34 g, 5.0 mmol) was dissolved in ethanol (50 mL) in an argon atmosphere. After the mixture had been stirred with K_2CO_3 (0.69 g, 5.0 mmol), 2-ethylhexyl bromide (0.9 mL, 5.0 mmol) was added. The reaction mixture was heated to reflux and stirred for 22 h. The reaction mixture was cooled to room temperature and evaporated in vacuo. The residue was dissolved in CH_2Cl_2, and the solution was washed twice with distilled water and once with brine. After drying over $MgSO_4$, the solution was filtered, and the solvent was evaporated in vacuo. After purification by column chromatography (silica gel, CH_2Cl_2/*n*-pentane 3:1), **2** was obtained as a brown oil. Yield: 0.54 g (28%); ^{1}H NMR ($CDCl_3$, 400 MHz): δ = 7.26 (s, 1H), 6.97 (s, 1H), 5.13 (s, 1H), 3.82 (d, J = 5.5 Hz, 2H), 1.75 (m, 1H), 1.60–1.40 (m, 4H), 1.40–1.25 (m, 4H), 0.94 (t, J = 7.5 Hz, 3H), 0.98 ppm (t, J = 7.0, 3H); ^{13}C NMR ($CDCl_3$, 75 MHz): δ = 150.27, 146.62, 120.25, 116.24, 112.42, 108.30, 72.54, 39.41, 30.45, 29.03, 23.87, 23.00, 14.06, 11.15 ppm; elemental analysis calcd (%) for $C_{14}H_{20}Br_2O_2$ (380.1): C 44.24, H 5.30; found: C 44.27, H 5.21.

***tert*-Butyl {(1*S*)-[2,5-Dibromo-4-(2-ethylhexyloxy)phenoxymethyl]-3-methylbutyl}carbamate (4)**: To a solution of ((*S*)-1-hydroxymethyl-3-methylbutyl)carbamic acid *tert*-butyl ester (**3**, 0.39 g, 1.79 mmol), compound **2** (0.69 g, 1.82 mmol), and triphenylphosphine (0.71 g, 2.71 mmol) in toluene (15 mL) under an argon atmosphere, a solution of diethyl azodicarboxylate (DEAD) (0.43 mL, 2.73 mmol) in toluene (5 mL) was added slowly so that the temperature of the reaction mixture did not exceed 35 °C. After stirring overnight at room temperature, the reaction mixture was filtered and washed with 1 M $KHSO_4$, distilled water and brine, and was subsequently dried over Na_2SO_4. After filtration and evaporation of the solvent in vacuo, the residue was purified by column chromatography (silica gel, ethyl acetate/*n*-heptane 1:4, R_f = 0.5). The product **4** was obtained as a clear sticky oil. Yield: 0.39 g (36%); ^{1}H NMR ($CDCl_3$, 400 MHz): δ = 7.07 (s, 1H), 7.00 (s, 1H), 4.79 (br d, 1H), 4.05–3.85 (m, 3H), 3.83 (d, J = 5.5 Hz, 2H), 1.80–1.60 (m, 2H), 1.60–1.20 (m, 10H), 1.45 (s, 9H), 1.00–0.85 ppm (m, 12H); ^{13}C NMR ($CDCl_3$, 75 MHz): δ = 155.38, 150.74, 149.56, 118.89, 117.95, 111.28, 111.17, 79.38, 72.49, 48.33, 40.96, 39.40, 30.49, 29.02, 28.40, 24.86, 23.85, 23.00, 22.90, 22.39, 14.06, 11.14 ppm; MALDI-TOF MS: m/z: 602.10 $[M+Na]^+$.

(1*S*)-[2,5-Dibromo-4-(2-ethylhexyloxy)phenoxymethyl]-3-methylbutylamine (5): To a solution of compound **4** (0.253 g, 0.44 mmol) in CH_2Cl_2 (4 mL), was added TFA (2.5 mL, 32 mmol). The mixture was stirred for 16 h under an argon atmosphere at room temperature. Subsequently, $NaHCO_3$ was added to the reaction mixture until the mixture became basic. After addition of CH_2Cl_2 (20 mL), the mixture was washed three times with distilled water and once with brine. After drying over Na_2SO_4, the solution was filtered, and the solvent was removed in vacuo to give a brown oil. Yield: 0.19 g (91%). The product was used without further purification. ^{1}H NMR ($CDCl_3$, 300 MHz): δ = 7.10 (s, 1H), 7.08 (s, 1H), 3.94 (dd, J = 8.5, 3.6 Hz, 1H), 3.83 (d, J = 5.5 Hz, 2H), 3.68 (t, J =

8.2 Hz, 1H), 3.30 (m, 1H), 1.85–1.60 (m, 4H), 1.60–1.40 (m, 4H), 1.40–1.25 (m, 6H), 1.00–0.85 ppm (m, 12H); ^{13}C NMR ($CDCl_3$, 75 MHz): δ = 150.65, 149.61, 118.84, 117.98, 111.23, 111.14, 75.77, 72.49, 48.70, 42.81, 39.41, 30.44, 29.03, 24.70, 23.86, 23.27, 23.00, 22.18, 14.06, 11.15 ppm; MALDI-TOF MS: m/z: 480.04 $[M+H]^+$.

***N*-(1-Ethylpropyl)perylene-3,4:9,10-tetracarboxylic-3,4-anhydride-9,10-imide (7)**: A mixture of *N*,*N*′-di(1-ethylpropyl)perylene-3,4:9,10-tertacarboxylic-bisimide (**6**, 2.87 g, 5.4 mmol) and potassium hydroxide (0.91 g, 0.016 mol) in *tert*-butyl alcohol (100 mL) was heated at 100 °C for 30 min. The reaction mixture was then poured into 10% HCl (400 mL), and the precipitate was filtered. The residue was stirred into a warm solution of potassium hydroxide (20 g, 0.36 mol) and potassium chloride (16 g, 0.21 mol) in water (200 mL). The solid was filtered and subsequently washed with the aqueous solution until the solution no longer had a yellow/green color. The solid was then stirred in water and subsequently filtered. The dark red filtrate was precipitated by addition of hydrochloric acid to a final total percentage of 10% HCl concentration. The precipitate was filtered, washed with water, and dried at 90 °C under vacuum to afford a black solid. Yield: 0.50 g (20%); ^{1}H NMR ($CDCl_3$) δ = 8.80–8.60 (m, 8H), 5.07 (m, 1H), 2.35–2.20 (m, 2H), 2.00–1.90 (m, 2H), 0.93 ppm (t, J = 7.5 Hz); ^{13}C NMR ($CDCl_3$) δ = 160.15, 136.61, 133.86, 133.76, 131.81, 124.10, 123.35, 123.24, 119.23, 58.03, 57.86, 25.16, 11.50 ppm; MS (EI): m/z: 461 $[M]^+$.

***N*-(1-Ethylpropyl)-*N*′-[(1*S*)-(2,5-dibromo-4-(2-ethylhexyloxy)phenoxymethyl)-3-methylbutyl] perylene-3,4:9,10-tetracarboxylic bisimide (8)**: Compound **5** (0.16 g, 0.33 mmol) and *N*-(1-ethylpropyl)perylene-3,4:9,10-tetracarboxylic-3,4-anhydride-9,10-imide (**7**, 0.15 g, 0.33 mmol) were stirred at 155 °C in DMF (20 mL) under an argon atmosphere for 24 h. The solvent was removed in vacuo, and the product was purified by column chromatography (silica gel, CH_2Cl_2) to afford a red solid. Yield: 0.12 g (39%); ^{1}H NMR ($CDCl_3$, 300 MHz): δ = 8.64 (d, J = 8.0 Hz, 4H), 8.56 (d, J = 8.0 Hz, 4H), 7.14 (s, 1H), 6.90 (s, 1H), 5.80 (m, 1H), 5.07 (m, 1H), 4.71 (t, J = 8.9 Hz, 1H), 4.34 (dd, J = 8.9, 5.6 Hz, 1H), 3.80–3.60 (m, 2H), 2.20–2.05 (m, 3H), 1.96 (m, 2H), 1.85–1.55 (m, 3H), 1.55–1.15 (m, 8H), 1.15–0.80 ppm (m, 18H); ^{13}C NMR ($CDCl_3$, 75 MHz): δ = 164.14, 150.57, 149.34, 134.57, 134.40, 131.98, 131.48, 129.55, 126.37, 124.83, 123.67, 123.05, 118.88, 117.78, 111.09, 72.39, 70.32, 57.73, 51.27, 39.33, 38.25, 30.36, 28.97, 25.61, 25.02, 23.79, 23.15, 22.96, 22.46, 14.02, 11.37, 11.10 ppm; MALDI-TOF MS: m/z: 921.90 $[M^{\bullet}]^-$; elemental analysis calcd (%) for $C_{49}H_{50}Br_2N_2O_6$ (922.8): C 63.78, H 5.46; found: C 63.14, H 5.41.

***tert*-Butyl [(1*S*)-(2,4-Dibromophenoxymethyl)3-methylbutyl]carbamate (10)**: ((*S*)-1-Hydroxymethyl-3-methylbutyl)carbamic acid *tert*-butyl ester (**3**, 1.017 g, 4.73 mmol), 2,4-dibromophenol (**9**, 1.19 g, 4.72 mmol), and triphenylphosphine (1.86 g, 7.09 mmol) were dissolved in toluene (15 mL), and stirred under an argon flux. A solution of DEAD (1.1 mL, 6.99 mmol) in toluene (10 mL) was added dropwise to the reaction mixture so that the temperature did not exceed 35 °C. After the mixture had been stirred overnight at room temperature, a white precipitate was filtered off from the reaction mixture. The remaining solution was washed with 1 M $KHSO_4$ (2×), with distilled water (3×), and with brine (1×). The organic phase was dried over Na_2SO_4, filtered, and the solvent was evaporated in vacuo. Cyclohexane and diethyl ether were added to the residue to yield a precipitate, which was filtered off. The solvents in the remaining solution were evaporated in vacuo. After purification by column chromatography (silica gel, ethyl acetate/*n*-heptane 1:4, R_f = 0.4) the product was crystallized from *n*-hexane. The product **10** was obtained as white crystals. Yield: 0.84 g (39%); ^{1}H NMR ($CDCl_3$, 300 MHz): δ = 7.66 (d, J = 2.2 Hz, 1H), 7.36 (dd, J = 8.9, 2.1 Hz, 1H), 6.76 (d, J = 8.8 Hz, 1H), 4.75 (br d, 1H), 4.05–3.90 (m, 3H), 1.70–1.60 (m, 1H), 1.60–1.40 (m, 2H), 1.44 (s, 9H), 0.96 ppm (dd, J = 6.4, 2.1 Hz, 6H); ^{13}C NMR ($CDCl_3$, 100 MHz): δ = 155.40, 154.47, 135.42, 131.27, 114.45, 113.23, 79.49, 71.50, 48.13, 40.93, 28.38, 24.85, 22.93, 22.31 ppm; MALDI-TOF MS: m/z: 474.08 $[M+Na]^+$.

(1*S*)-(2,4-Dibromophenoxymethyl)-3-methylbutylamine (11): A solution of compound **10** (0.76 g, 1.68 mmol) in CH_2Cl_2 (5 mL) and was stirred with TFA (5 mL, 65 mmol) under argon. After 15 h, $NaHCO_3$ was added to the reaction mixture until it was basic. The mixture was subsequently washed with distilled water (4×) and with brine (1×). The solution was dried over Na_2SO_4, and after filtration and evaporation in vacuo, **11** was obtained as a pink oil. Yield: 0.49 g (83%). The product was used without any further purification. ^{1}H NMR ($CDCl_3$, 300 MHz): δ = 7.66 (d, J = 2.5 Hz, 1H), 7.35 (dd, J = 8.8, 2.5 Hz, 1H), 6.75 (d, J = 8.8 Hz, 1H), 3.96 (dd, J = 8.8, 3.6 Hz, 1H), 3.70 (dd, J = 8.7, 7.6 Hz, 1H), 3.30 (m, 1H), 1.79 (m, 1H), 1.34 (t, J = 7.0 Hz, 2H), 0.96 ppm (t, J = 6.7 Hz, 6H); ^{13}C NMR ($CDCl_3$, 100 MHz): δ = 154.56, 135.42, 131.21, 114.40, 113.18, 113.06, 75.10, 48.48, 43.06, 24.70, 23.36, 22.11 ppm; MALDI-TOF MS: m/z: 351.85 $[M+H]^+$.

***N*-(1-Ethylpropyl)-*N*′-[(1*S*)-(2,4-dibromophenoxymethyl)-3-methylbutyl]-perylene-3,4:9,10-tetracarboxylic bisimide (12)**: Compound **11** (0.34 g, 0.97 mmol) and *N*-(1-ethylpropyl)perylene-3,4:9,10-tetracarboxylic-3,4-anhydride-9,10-imide (**7**, 0.45 g, 0.98 mmol) were stirred in DMF (25 mL) at 140 °C under an argon atmosphere. After 2.5 h, the temperature was elevated to 160 °C. After subsequent 17 h of stirring, the reaction mixture was cooled to room temperature, and the solvent was evaporated in vacuo. After purification by column chromatography (silica gel, CH_2Cl_2), **12** was obtained as a red solid. Yield: 0.53 g (69%); ^{1}H NMR ($CDCl_3$, 300 MHz): δ = 8.80–8.60 (m, 8H), 7.51 (d, J = 2.5 Hz, 1H), 7.34 (dd, J = 8.7, 2.3 Hz, 1H), 6.80 (d, J = 8.8 Hz, 1H), 5.83 (m, 1H), 5.07 (m, 1H), 4.73 (t, J = 8.9 Hz, 1H), 4.39 (dd, J = 9.1, 5.8 Hz, 1H), 2.28 (m, 3H), 1.95 (m, 2H), 1.78 (m, 1H), 1.67 (m, 1H), 1.02 (dd, J = 13.6, 6.5 Hz, 6H), 0.93 ppm (t, J = 7.4 Hz, 6H); ^{13}C NMR ($CDCl_3$, 75 MHz): δ = 164.00, 154.24, 135.29, 134.73, 134.44, 131.65, 131.16, 129.61, 126.45, 123.50, 123.14, 114.59, 113.17, 69.44, 57.72, 50.97, 38.17, 25.58, 25.01, 23.15, 22.41, 11.34 ppm; MALDI-TOF MS: m/z: 793.88 $[M^{\bullet}]^-$; elemental analysis calcd (%) for $C_{41}H_{34}Br_2N_2O_5$ (794.6): C 61.98, H 4.31; found: C 61.76, H 4.23.

2,4-Dibromo-1-(2-ethylhexyloxy)benzene (13): To a stirred solution of 2,4-dibromophenol (**9**, 1.03 g, 4.09 mmol) in ethanol (25 mL), was added K_2CO_3 (0.57 g, 4.12 mmol) and subsequently 2-ethylhexyl bromide (0.73 mL, 4.10 mmol) under an argon atmosphere. After refluxing for 2 h, the reaction mixture was cooled to room temperature, and the solvent was evaporated in vacuo. The residue was dissolved in CH_2Cl_2 and washed with 1 M NaOH, distilled water, and brine and dried over Na_2SO_4. Purification by column chromatography (silica gel, CH_2Cl_2), followed by evaporation of the solvent, gave a residue that was heated at 80 °C in vacuo. The resulting product was obtained as a clear liquid. Yield: 0.36 g (24%); ^{1}H NMR ($CDCl_3$, 300 MHz): δ = 7.65 (d, J = 2.5 Hz, 1H), 7.34 (dd, J = 8,7, 2.3 Hz, 1H), 6.75 (d, J = 8.8 Hz, 1H), 3.87 (d, J = 5.8 Hz, 2H), 1.77 (m, 1H), 1.60–1.40 (m, 4H), 1.40–1.20 (m, 4H), 1.00–0.85 ppm (m, 6H); ^{13}C NMR ($CDCl_3$, 75 MHz): δ = 155.02, 135.37, 131.06, 114.08, 113.17, 112.47, 71.75, 39.31, 30.45, 29.03, 23.87, 22.99, 14.05, 11.14 ppm; elemental analysis calcd (%) for $C_{14}H_{20}Br_2O$ (364.1): C 46.18, H 5.54; found: C 45.64, H 5.36.

P1: A mixture of monomer **8** (0.040 g, 0.043 mmol), monomer (*E*,*E*)-1,4-bis{4-[4,4,5,5-tetramethyl[1,3,2]dioxaborolan-2-yl-}-2,5-bis[(*S*)-2-methylbutoxy]styryl}-2,5-bis[(*S*)-2-methylbutoxy]benzene (**14**, 0.0456 g, 0.043 mmol), and $[Pd(PPh_3)_4]$ (0.0025 g, 0.002 mmol) in distilled THF (10 mL) was purged with argon for 15 min. A solution of K_2CO_3 (0.024 g, 0.17 mmol) in water (1.2 mL), which had also been purged with argon for 15 min, was added to this mixture with a syringe. The whole mixture was purged with argon for 15 min before stirring in the dark at 90 °C under a flow of argon. After 22 h, the reaction mixture was cooled to room temperature, and dried in vacuo. The residue was dissolved in toluene (3 mL). Methanol (300 mL) was added and the precipitated solid was filtered. Yield: 0.048 g (72%) of a red solid; ^{1}H NMR ($CDCl_3$, 300 MHz): δ = 8.80–8.10 (m, 8H), 7.70–6.40 (m, 12H), 5.90–5.60 (br signal, 1H), 5.10–4.90 (m, 1H), 4.80–4.50 (br signal, 1H), 4.50–4.10 (br signal, 1H), 4.00–3.20 (m, 14H), 2.40–1.20 (m, 34H), 1.20–1.10 (m, 6H), 1.10–0.70 ppm (m, 48H); ^{13}C NMR ($CDCl_3$, 75 MHz): δ = 163.98, 163.53, 150.96, 150.61, 150.39, 149.61, 149.43, 134.56, 134.22, 131.42, 130.42, 129.62, 129.42, 129.26, 128.43, 127.62, 127.14, 126.78, 126.32, 125.28, 123.62, 123.02, 122.40, 117.10, 116.69, 115.80, 110.90, 110.39, 110.06, 108.67, 74.43, 73.81, 71.81, 57.54, 51.07, 39.53, 38.14, 35.12, 34.89, 30.47, 29.02, 26.40, 26.19, 26.02, 25.57, 25.01, 23.83, 23.15, 23.00, 22.57, 16.83, 16.70, 14.03, 11.48, 11.39, 11.32, 10.97 ppm; SEC ($CHCl_3$, versus polystyrene): M_w = 27.2 kg mol^{-1}, M_n = 8.2 kg mol^{-1}.

P2: Monomer **12** (0.151 g, 0.19 mmol), monomer **14** (0.200 g, 0.19 mmol), and $[Pd(PPh_3)_4]$ (0.009 g, 0.008 mmol) in distilled THF (30 mL) were purged with argon for 20 min. A solution of K_2CO_3 (0.10 g, 0.72 mmol) in water (5 mL) was purged for 30 min, and this solution was added to the THF solution with a syringe. The whole solution was again purged with

argon for 30 min. The reaction mixture was heated to 90 °C, and was stirred under an argon atmosphere in the dark for 18 h. After the mixture was cooled to room temperature, the solvents were evaporated in vacuo. The residue was dissolved in $CHCl_3$ (7 mL), and methanol (500 mL) was added. The resulting precipitate was filtered off, and the filtrate was dried in vacuo. The precipitation procedure was repeated from toluene (4 mL) in methanol (250 mL). The polymer was obtained as a red solid. Yield: 0.202 g (75 %); ^{1}H NMR ($CDCl_3$, 400 MHz): δ = 8.80–8.05 (m, 8H), 7.70–6.70 (m, 13H), 5.95–5.65 (br signal, 1H), 5.20–4.90 (br signal, 1H), 4.80–4.60 (m, 1H), 4.60–4.30 (br signal, 1H), 4.10–3.00 (m, 12H), 2.30–0.60 ppm (m, 73H); ^{13}C NMR ($CDCl_3$, 100 MHz): δ = 163.96, 150.94, 134.60, 132.00, 130.39, 129.40, 127.78, 126.32, 123.66, 123.12, 122.38, 115.57, 110.31, 109.99, 108.72, 74.51, 74.22, 57.50, 50.73, 38.08, 35.10, 34.95, 34.80, 30.92, 26.34, 26.17, 25.94, 25.54, 25.02, 23.10, 22.53, 16.78, 16.32, 11.43 ppm; SEC ($CHCl_3$, versus polystyrene): M_w = 22.2 kg mol^{-1}, M_n = 8.0 kg mol^{-1}.

RP1: A solution of 1,4-dibromo-2,5-di-(2-ethylhexyloxy)benzene (**15**, 0.018 g, 0.037 mmol), **14** (0.038 g, 0.036 mmol), and [Pd(PPh_3)$_4$] (0.002 g, 0.001 mmol) in distilled THF (7 mL) was purged with argon for 15 min. A solution of K_2CO_3 (0.020 g, 0.14 mmol) in water (1 mL), which had also been purged with argon for 15 min, was added to this mixture with a syringe. This whole solution was purged with argon for 15 min. The temperature was elevated to 90 °C, and the reaction mixture was stirred for 23 h in the dark. After the mixture was cooled to room temperature, the solvents were evaporated in vacuo. The residue was dissolved in toluene (4 mL) and poured into methanol (300 mL). The precipitate was filtered off and was washed with water and methanol to afford a yellow solid. Yield: 0.021 g (51 %); ^{1}H NMR ($CDCl_3$, 400 MHz): δ = 7.57 (brs, 4H), 7.40–7.20 (brs, 4H), 7.01 (s, 2H), 6.98 (s, 2H), 4.00–3.60 (m, 16H), 2.05–1.85 (brs, 4H), 1.85–1.05 (m, 36H), 1.05–0.75 ppm (m, 48H); ^{13}C NMR ($CDCl_3$, 100 MHz): δ = 151.08, 150.95, 150.36, 150.13, 127.55, 123.11, 122.50, 117.10, 110.47, 110.07, 74.38, 74.30, 71.88, 39.57, 35.09, 34.90, 30.54, 29.70, 29.04, 26.39, 26.12, 23.85, 23.02, 16.82, 16.72, 14.07, 11.47, 11.28, 11.00 ppm; SEC ($CHCl_3$, versus polystyrene): M_w = 110.8 kg mol^{-1}, M_n = 24.6 kg mol^{-1}.

RP2: Monomer **13** (0.0279 g, 0.077 mmol), monomer **14** (0.0805 g, 0.077 mmol), and [Pd(PPh_3)$_4$] (0.0035 mg, 0.003 mmol) were dissolved in distilled THF (13 mL) and the solution was purged with argon for 20 min. A solution of K_2CO_3 (0.04 g, 0.029 mmol) in water (2 mL) was purged with argon for 15 minutes and was subsequently added to the organic solution. The reaction mixture was purged with argon for 30 minutes before heating to 90 °C. After stirring in the dark for 18 h, the reaction mixture was dried by evaporation in vacuo. The solid residue was washed with water (2×) and then dissolved in toluene (4 mL). The solution was poured in methanol (100 mL), and the precipitate was filtered off to give a yellow solid. Yield: 0.042 g (55 %); ^{1}H NMR (CD_2Cl_2, 300 MHz): δ = 7.60–7.40 (m, 6H), 7.30–7.05 (m, 4H), 7.00–6.80 (m, 3H), 4.00–3.80 (m, 14H), 1.95 (m, 4H), 1.80 (m, 2H), 1.75–1.20 (m, 21H), 1.20–0.70 ppm(m, 42H); ^{13}C NMR (CD_2Cl_2, 100 MHz): δ = 156.29, 151.45, 151.36, 150.79, 134.40, 132.71, 131.03, 130.19, 129.19, 127.82, 126.77, 126.51, 123.25, 122.69, 117.02, 115.76, 112.60, 111.61, 110.27, 110.11, 74.81, 74.71, 74.27, 71.23, 39.77, 35.40, 35.25, 35.17, 30.83, 29.35, 26.67, 26.47, 26.38, 24.16, 23.33, 16.87, 16.60, 14.14, 11.55, 11.30, 11.14 ppm; SEC ($CHCl_3$, versus polystyrene): M_w = 48.8 kg mol^{-1}, M_n = 13.8 kg mol^{-1}.

Acknowledgement

The authors would like to thank E. H. A. Beckers, Dr. S. C. J. Meskers, and Dr. M. M. Wienk for measurements and helpful discussions. This work was financially supported by the Council for Chemical Sciences of the Netherlands Organization for Scientific Research (CW-NWO) and the Eindhoven University of Technology in the PIONIER program (98400).

[1] C. Ego, D. Marsitzky, S. Becker, J. Zhang, A. C. Grimsdale, K. Müllen, J. D. MacKenzie, C. Silva, R. H. Friend, *J. Am. Chem. Soc.* **2003**, *125*, 437.
[2] F. Jäckel, S. De Feyter, J. Hofkens, F. Köhn, F. C. De Schryver, C. Ego, A. Grimsdale, K. Müllen, *Chem. Phys. Lett.* **2002**, *362*, 534.
[3] L. M. Herz, C. Silva, R. H. Friend, R. T. Philips, S. Setayesh, S. Becker, D. Marsitsky, K. Müllen, *Phys. Rev. B* **2001**, *64*, 195203.
[4] D. Beljonne, G. Pourtois, C. Silva, E. Hennebicq, L. M. Herz, R. H. Friend, G. D. Scholes, S. Setayesh, K. Müllen, J. L. Brédas, *Proc. Natl. Acad. Sci. USA* **2002**, *99*, 10982.
[5] D. M. Russell, A. C. Arias, R. H. Friend, C. Silva, C. Ego, A. C. Grimsdale, K. Müllen, *Appl. Phys. Lett.* **2002**, *80*, 2204.
[6] B. de Boer, U. Stalmach, P. F. van Hutten, C. Melzer, V. V. Krasnikov, G. Hadziioannou, *Polymer* **2001**, *42*, 9097.
[7] U. Stalmach, B. de Boer, C. Videlot, P. F. van Hutten, G. Hadziioannou, *J. Am. Chem. Soc.* **2000**, *122*, 5464.
[8] A. Cravino, N. S. Sariciftci, *J. Mater. Chem.* **2002**, *12*, 1931.
[9] T. Benincori, E. Brenna, F. Sannicolò, L. Trimarco, G. Zotti, P. Sozzani, *Angew. Chem.* **1996**, *108*, 718; *Angew. Chem. Int. Ed. Engl.* **1996**, *35*, 648.
[10] J. P. Ferraris, A. Yassar, D. C. Loveday, M. Hmyene, *Opt. Mater.* **1998**, *9*, 34.
[11] A. Cravino, G. Zerza, M. Maggini, S. Bucella, M. Svensson, M. R. Andersson, H. Neugebauer, N. S. Sariciftci, *Chem. Commun.* **2000**, 2487.
[12] A. Cravino, G. Zerza, H. Neugebauer, M. Maggini, S. Bucella, E. Menna, M. Svensson, M. R. Andersson, C. J. Brabec, N. S. Sariciftci, *J. Phys. Chem. B* **2002**, *106*, 70.
[13] A. Marcos Ramos, M. T. Rispens, J. K. J. van Duren, J. C. Hummelen, R. A. J. Janssen, *J. Am. Chem. Soc.* **2001**, *123*, 6714.
[14] F. Zhang, M. Svensson, M. R. Andersson, M. Maggini, S. Bucella, E. Menna, O. Inganäs, *Adv. Mater.* **2001**, *13*, 1871.
[15] S. Wang, S. Xiao, Y. Li, Z. Shi, C. Du, H. Fang, D. Zhu, *Polymer* **2002**, *43*, 2049.
[16] S. Xiao, S. Wang, H. Fang, Y. Li, Z. Shi, C. Du, D. Zhu, *Macromol. Rapid Commun.* **2001**, *22*, 1313.
[17] G. Zerza, A. Cravino, H. Neugebauer, N. S. Sariciftci, R. Gómez, J. L. Segura, N. Martín, M. Svensson, M. R. Andersson, *J. Phys. Chem. A* **2001**, *105*, 4172.
[18] F. Giacalone, J. L. Segura, N. Martín, M. Catellani, S. Luzzati, N. Lupsac, *Org. Lett.* **2003**, *5*, 1669.
[19] A. Herrmann, T. Weil, V. Sinigersky, U.-M. Wiesler, T. Vosch, J. Hofkens, F. C. De Schryver, K. Müllen, *Chem. Eur. J.* **2001**, *7*, 4844.
[20] M. Lor, J. Thielemans, L. Viaene, M. Cotlet, J. Hofkens, T. Weil, C. Hampel, K. Müllen, J. W. Verhoeven, M. Van der Auweraer, F. C. De Schryver, *J. Am. Chem. Soc.* **2002**, *124*, 9918.
[21] M. Lor, S. Jordens, G. De Belder, G. Schweitzer, E. Fron, L. Viaene, M. Cotlet, T. Weil, K. Müllen, J. W. Verhoeven, M. Van der Auweraer, F. C. De Schryver, *Photochem. Photobiol. Sci.* **2003**, *2*, 501.
[22] F. Würthner, A. Sautter, *Chem. Commun.* **2000**, 445.
[23] F. Würthner, A. Sautter, *Org. Biomol. Chem.* **2003**, *1*, 240.
[24] C.-C. You, F. Würthner, *J. Am. Chem. Soc.* **2003**, *125*, 9716.
[25] F. Würthner, A. Sautter, D. Schmid, P. J. A. Weber, *Chem. Eur. J.* **2001**, *7*, 894.
[26] E. E. Neuteboom, S. C. J. Meskers, P. A. van Hal, J. K. J. van Duren, E. W. Meijer, R. A. J. Janssen, H. Dupin, G. Pourtois, J. Cornil, R. Lazzaroni, J.-L. Brédas, D. Beljonne, *J. Am. Chem. Soc.* **2003**, *125*, 8625.
[27] R. S. Lokey, B. L. Iverson, *Nature* **1995**, *375*, 303.
[28] E. Peeters, P. A. van Hal, S. C. J. Meskers, R. A. J. Janssen, E. W. Meijer, *Chem. Eur. J.* **2002**, *8*, 4470.
[29] T. Vahlenkamp, G. Wegner, *Macromol. Chem. Phys.* **1994**, *195*, 1933.
[30] S. Demmig, H. Langhals, *Chem. Ber.* **1988**, *121*, 225.
[31] H. Kaiser, J. Lindner, H. Langhals, *Chem. Ber.* **1991**, *124*, 529.
[32] Y. Nagao, T. Naito, Y. Abe, T. Misono, *Dyes Pigm.* **1996**, *32*, 71.
[33] A. P. Monkman, L.-O. Pålsson, R. W. T. Higgins, C. Wang, M. R. Bryce, A. S. Batsanov, J. A. K. Howard, *J. Am. Chem. Soc.* **2002**, *124*, 6049.
[34] A. L. Ding, J. Pei, Z. K. Chen, Y. H. Lai, W. Huang, *Thin Solid Films* **2000**, *363*, 114.
[35] E. Peeters, A. Delmotte, R. A. J. Janssen, E. W. Meijer, *Adv. Mater.* **1997**, *9*, 493.
[36] A. Weller, *Z. Phys. Chem. Neue Folge* **1982**, *133*, 93.
[37] E. Hädicke, F. Graser, *Acta Crystallogr. Sect. C* **1986**, *42*, 189.

[38] E. Peeters, P. A. van Hal, J. Knol, C. J. Brabec, N. S. Sariciftci, J. C. Hummelen, R. A. J. Janssen, *J. Phys. Chem. B* **2000**, *104*, 10174.
[39] J. Salbeck, *J. Electroanal. Chem.* **1992**, *340*, 169.
[40] P. A. van Hal, E. H. A. Beckers, E. Peeters, J. J. Apperloo, R. A. J. Janssen, *Chem. Phys. Lett.* **2000**, *328*, 403.
[41] P. A. van Hal, M. P. T. Christiaans, M. M. Wienk, J. M. Kroon, R. A. J. Janssen, *J. Phys. Chem. B* **1999**, *103*, 4352.

Received: January 31, 2004
Published online: June 24, 2004